

Cobalt Carbonyl Nitrosyl Complexes: Matrix Infrared Spectra and Density Functional Calculations

Xuefeng Wang and Lester Andrews*

Department of Chemistry, University of Virginia, Charlottesville, Virginia 22904-4319

Received: November 30, 2000; In Final Form: February 16, 2001

Reactions of laser-ablated cobalt atoms with CO and NO mixtures in excess argon during condensation at 7 K generate a series of unsaturated cobalt carbonyl nitrosyls including $\text{Co}(\text{CO})(\text{NO})$, $\text{Co}(\text{CO})[\text{NO}]$, $\text{OCo}(\text{NCO})$, $\text{Co}(\text{CO})_2(\text{NO})$, $\text{Co}(\text{CO})_2[\text{NO}]$, and $\text{Co}(\text{CO})(\text{NO})_2$, and the saturated $\text{Co}(\text{CO})_3(\text{NO})$ molecule. The observed infrared bands of reaction products are identified by isotopic substitution, isotopic ratios, and isotopic distributions (^{13}C , ^{15}N , ^{18}O , and mixtures). DFT/BPW91 vibrational fundamental calculations reproduced the observed frequencies and isotopic shifts very well. The isocyanate $\text{OCo}(\text{NCO})$ is formed from the side-bonded $\text{Co}[\text{NO}]$ reaction with CO, which is relevant to catalytic reduction processes.

Introduction

Transition-metal reactions with nitrogen oxides continue to be of interest due to the photocatalytic properties and thermal decompositions of metal nitrosyls.^{1,2} The NO_x species can be converted to N_2 and O_2 through the reaction between NCO species and NO by catalytic reduction, which is very important in organometallic chemistry and air pollution control.^{3–10} The study of reduction of NO by CO on several metal surfaces has been achieved through molecular beams in conjunction with mass spectrometry, as well as the in situ infrared couples with temperature-programmed reaction techniques.^{9,10} Recent laser-ablation investigations of manganese and iron atom reactions with NO and CO mixtures revealed that several unsaturated metal carbonyl nitrosyl complexes and isocyanate were formed as reaction products.^{11,12}

The saturated 18-electron tricarbonylnitrosylcobalt ($\text{Co}(\text{CO})_3\text{NO}$) has been synthesized, and its structure, spectra, ion–molecule chemistry, and photochemistry have been investigated.^{13–17} The unsaturated $\text{Co}(\text{CO})_2\text{NO}$ species was produced by UV photolysis of $\text{Co}(\text{CO})_3\text{NO}$ in solid argon,¹³ and $\text{Co}(\text{CO})_2(\text{NO})(\text{H}_2)$ was formed with hydrogen in liquid xenon.¹⁷ The 248-nm laser photolysis of $\text{Co}(\text{CO})_3\text{NO}$ in the gas phase gave a series of sequential ligand eliminations to leave CoCO , which reacts back with parent $\text{Co}(\text{CO})_3\text{NO}$ to form $\text{Co}_2(\text{CO})_4(\text{NO})$.¹⁵ However, there have not been, to the best of our knowledge, other studies on the unsaturated cobalt carbonyl nitrosyl complexes. In fact, such unstable species are frequently related to intermediates involved in catalytic processes. This report of our ongoing investigations of laser-ablated metal atom reactions with small molecules focuses on cobalt atoms with CO and NO mixtures in excess argon during condensation at 7 K. The vibrational frequencies and structures of various cobalt carbonyl nitrosyls are determined using isotopic substitution in the infrared spectra and density functional theory (DFT) calculations. We also expect to gain a better understanding of NO + CO reactions with metals that may assist in the catalytic removal of automobile exhaust gases.

Experimental Section

The experiments for reactions of laser-ablated metal atoms with small molecules during condensation in excess argon has been described in detail previously.¹⁸ The Nd:YAG laser fundamental (1064 nm, 10 Hz repetition rate with 10 ns pulse width) was focused onto a rotating cobalt target (Johnson Matthey). The laser energy was varied from 5 to 40 mJ/pulse. Laser-ablated cobalt atoms were co-deposited with nitric oxide and carbon monoxide mixture (0.2 to 0.5%) in excess argon onto a 7 K CsI cryogenic window at 2–4 mmol/h for 1 h. Isotopic $^{13}\text{C}^{16}\text{O}$, $^{15}\text{N}^{16}\text{O}$, and $^{15}\text{N}^{18}\text{O}$, and selected mixtures were used in different experiments. FTIR spectra were recorded at 0.5 cm^{-1} resolution on Nicolet 750 with 0.1 cm^{-1} accuracy using an MCTB detector. Matrix samples were annealed at different temperatures, and selected samples were subjected to broadband photolysis by a medium-pressure mercury arc lamp (Philips, 175W) with globe removed.

Results

Infrared spectra are presented for reaction products of laser-ablated cobalt atoms with CO and NO mixtures. For comparison, the infrared spectra and structures of various cobalt carbonyl nitrosyl complexes are reproduced by theoretical calculations.

Spectra of Reaction Products. The infrared spectra of laser-ablated cobalt atom co-deposition with 0.2% CO + 0.2% NO in excess argon are shown in Figure 1, and the absorptions are listed in Table 1. Bands due to CO, NO, *cis*-(NO)₂ and other common species including N_2O , NO_2 , $(\text{NO})_2^+$, NO_2^- , and $(\text{NO})_2^-$ were also observed.^{11,12,20} After deposition, weak bands appeared at 2250.1, 2000.9, 1767.9, 1761.1, 1737.6, 1324.1, and 1284.2 cm^{-1} . Weak bands at 1960.5, 1920.8, and 1983.3 cm^{-1} have been identified as $\text{Co}(\text{CO})$, $\text{Co}(\text{CO})_2$, and $\text{Co}(\text{CO})_3$, respectively.¹⁹ The 1761.1 and 1737.6 cm^{-1} bands are due to the $\text{Co}(\text{NO})$ and $\text{Co}(\text{NO})_2$ species.²⁰ Stepwise annealing to 20 and 30 K decreased bands due to CO (2138.2 cm^{-1}) and NO (1871.8 cm^{-1}), but increased the weak bands observed after deposition, and produced new bands at 2106.8, 2071.2, 2039.4, 2010.1, 1787.9, 1770.1, 1719.7, and 1346.7 cm^{-1} ; the 1770.1 cm^{-1} band is due to $\text{Co}(\text{NO})_3$.¹⁹ A 10-min broadband photolysis decreased absorptions at 2078.4, 2010.1, and 1346.7 cm^{-1} , and

* To whom correspondence should be addressed. E-mail: isa@virginia.edu.

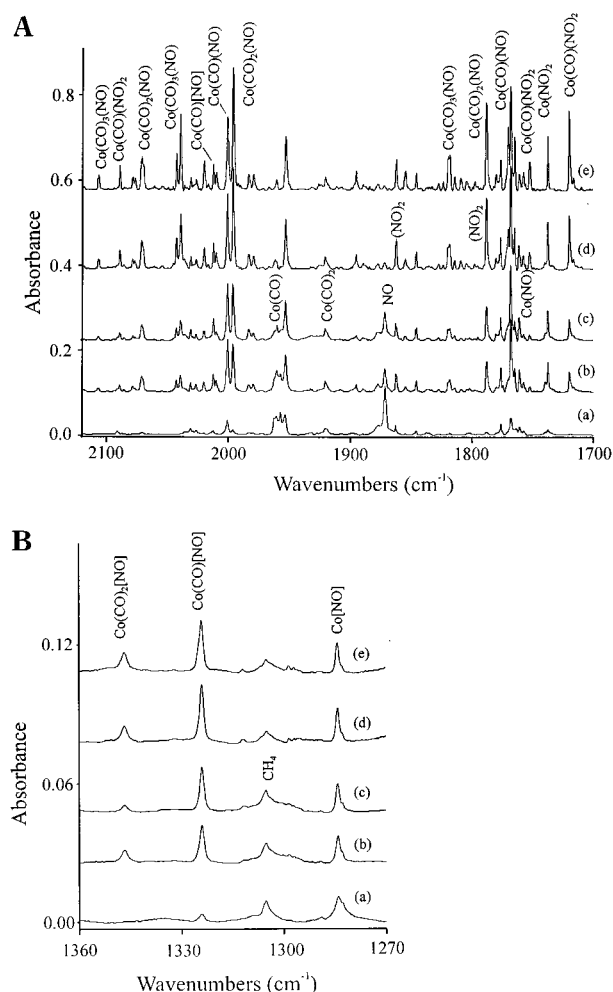


Figure 1. Infrared spectra in the (A) 2120–1700 and (B) 1360–1270 cm^{-1} regions for laser-ablated Co atoms co-deposited with 0.2% CO + 0.2% NO in argon at 7 K: (a) after 1 h sample deposit, (b) after annealing to 30 K, (c) after $\lambda > 240$ nm photolysis for 10 min, (d) after annealing to 35 K, and (e) after annealing to 40 K.

a final 40 K annealing increased the 2078.4, 2010.1, and 1346.7 cm^{-1} bands and other absorptions.

The isotopic $^{13}\text{C}^{16}\text{O} + ^{14}\text{N}^{16}\text{O}$, $^{12}\text{C}^{16}\text{O} + ^{15}\text{N}^{16}\text{O}$, and $^{12}\text{C}^{16}\text{O} + ^{15}\text{N}^{18}\text{O}$ spectra were also recorded and listed in Table 1. Spectra of $^{12}\text{C}^{16}\text{O} + ^{13}\text{C}^{16}\text{O} + ^{14}\text{N}^{16}\text{O}$ and $^{12}\text{C}^{16}\text{O} + ^{14}\text{N}^{16}\text{O} + ^{15}\text{N}^{16}\text{O}$ mixtures shown in Figures 2 and 3 were used for molecule identifications.

Calculations. The density functional theory calculations performed in this study employed the GAUSSIAN 94 program.²¹ All equilibrium geometries were fully optimized using the BPW91 density functional (Becke exchange with Perdew and Wang correlation functional), 6-311+G(d) basis set for C, N and O,^{22,23} and the all-electron set of Wachters and Hay as modified for cobalt atoms.²⁴ All geometrical parameters were fully optimized, and the harmonic vibrational frequencies were obtained analytically at the optimized structures. The computed geometry parameters, relative energies and frequencies, intensities, and isotopic frequency ratios for various unsaturated cobalt carbonyl nitrosyl complexes are summarized in Table 2 and Table 3, while results for the saturated 18-electron molecule, $\text{Co}(\text{CO})_3(\text{NO})$, are listed in Table 4.

Five isomers are located on the potential energy hypersurface of CoCONO . The ground $^1A'$ state of the $\text{Co}(\text{CO})(\text{NO})$ complex, in which both CO and NO bond to Co with end-on coordination, is the global minimum at this level of theory, and the $^3A''$ state

is 19.0 kcal/mol higher in energy. The next isomer, $\text{Co}(\text{CO})(\eta^2\text{-NO})$ with 1A symmetry, is 26.0 kcal/mol higher in energy than $\text{Co}(\text{CO})(\text{NO})$ ($^1A'$). The NO bond length for this molecule is 1.229 Å, much longer than in $\text{Co}(\text{CO})(\text{NO})$ (1.175 Å), indicating a NO side-on interaction with the Co atom. The linear molecules, $\text{OC}(\text{NO})\text{Co}$ and $\text{OC}(\text{NO})\text{Co}$, with $^1\Sigma$ ground states, are isocyanate NCO bonded to CoO, and 26.4 and 52.6 kcal/mol, respectively, above the ground-state $\text{Co}(\text{CO})(\text{NO})$ molecule. The $\text{NCoO}(\text{CO})$ isomer, described as CoCO inserted into NO, is 42.5 kcal/mol higher in energy.

Both $\text{Co}(\text{CO})_2(\text{NO})$ and $\text{Co}(\text{CO})_2(\eta^2\text{-NO})$ are calculated to have singlet ground states, but the former is 14.5 kcal/mol lower in energy. The $\text{Co}(\text{CO})_3(\text{NO})$ molecule is found to have a singlet ground state with C_{3v} symmetry. The calculated parameters are in good agreement with electron diffraction structure determinations.²⁵

Finally, BPW91 calculations were also done for $\text{Co}(\text{CO})_x$ ($x = 1, 2$) and $\text{Co}(\text{NO})_x$ ($x = 1, 2$) to compare calculated frequencies with the experimental values. The CO stretching mode in $\text{Co}(\text{CO})$ and antisymmetric vibration in $\text{Co}(\text{CO})_2$ are predicted at 1985.4 and 1934.1 cm^{-1} , respectively, which are only 1.4 and 0.7% higher than argon matrix measurements.¹⁹ However, the predicted 1836.5 and 1773.5 cm^{-1} NO stretching modes in $\text{Co}(\text{NO})$ and $\text{Co}(\text{NO})_2$ are overestimated by 4.3 and 2.1% compared with our argon matrix data.²⁰ As will be discussed below, the calculated CO stretching frequencies and intensities in several cobalt carbonyl nitrosyls are in excellent agreement with the experimental observations, but the NO stretching frequencies are overestimated, which are systematic discrepancies.

Discussion

Seven sets of new reaction product absorptions will be assigned to cobalt carbonyl nitrosyl complexes on the basis of annealing and photolysis behavior, isotopic substitution, and DFT isotopic frequency calculations. The $\text{Co}(\text{CO})_x$ and $\text{Co}(\text{NO})_x$ complexes identified in early works from this group^{19,20} are listed in Table 1.

$\text{Co}(\text{CO})(\text{NO})$. The bands at 2000.9 and 1767.9 cm^{-1} can be assigned to the $\text{Co}(\text{CO})(\text{NO})$ complex. These two bands appeared after deposition, increased on annealing, and maintained an 0.8 relative absorbance. The 2000.9 cm^{-1} band shifts to 1956.4 cm^{-1} in the $^{13}\text{CO} + \text{NO}$ experiment (1.0227 $^{12}\text{C}/^{13}\text{C}$ isotopic ratio) but shows a 1.4 cm^{-1} ^{15}NO isotopic shift, suggesting a C–O stretching mode weakly coupled to nitrogen. However, the 1767.9 cm^{-1} band exhibits large (1.0201) $^{14}\text{N}/^{15}\text{N}$ but small (1.0009) $^{12}\text{C}/^{13}\text{C}$ isotopic ratios, indicating an N–O stretching mode with little effect from carbon. In the mixed $^{12,13}\text{CO} + \text{NO}$ and $\text{CO} + ^{14,15}\text{NO}$ experiments doublet isotopic structures were observed, showing that only one CO as well as one NO subunit are involved in this molecule.

DFT calculations support this assignment. As listed in Table 3, the C–O stretching frequency of $\text{Co}(\text{CO})(\text{NO})$ ($^1A'$) is predicted at 2000.2 cm^{-1} , only 0.7 cm^{-1} from the experimental observation. The calculated N–O stretching mode at 1807.0 cm^{-1} is 39.1 cm^{-1} higher than the observed value. The predicted relative intensity (591/984 = 0.60) and isotopic frequency ratios of the two bands match the experimental values very well.

$\text{Co}(\text{CO})[\text{NO}]$ or $\text{Co}(\text{CO})(\eta^2\text{-NO})$. The 1300 cm^{-1} region contains product bands at 1284.1 and 1324.1 cm^{-1} . The stronger 1284.1 cm^{-1} band shows a sharp doublet with $\text{Co} + ^{14,15}\text{NO}$, and it has been assigned to side-bound $\text{Co}[\text{NO}]$.²⁰ The present BPW91 calculations predict a strong N–O stretching mode for this $^1A'$ species at 1350.7 cm^{-1} with $^{14}\text{NO}/^{15}\text{NO}$ and $^{15}\text{N}^{16}\text{O}/$

TABLE 1: Absorptions (cm⁻¹) from Co-Deposition of Laser-Ablated Co Atoms with NO and CO in Argon at 7 K

CO + NO	¹³ CO + NO	CO + ¹⁵ NO	CO + ¹⁵ N ¹⁸ O	^{12,13} CO + NO	CO + ^{14,15} NO	¹² CO/ ¹³ CO	¹⁴ NO/ ¹⁵ NO	assignment
2250.1	2189.4	2236.8	2236.8	2250.1, 2189.4	2250.0, 2236.8	1.0277	1.0059	OCo(NCO)
2106.8	2059.3	2106.0	2105.3	2106.7, 2083.3, 2059.3	2106.8	1.0231	1.0004	Co(CO) ₃ (NO)
2089.0	2042.6	2087.6	2087.3	2089.3, 2042.6	2088.5	1.0227	1.0008	Co(CO)(NO) ₂
2078.4	2030.9	2078.0	2077.3	2078.6, (2054.5), 031.0	2078.4	1.0234	1.0002	Co(CO) ₂ [NO]
2071.2	2024.8	2070.2	2069.3	2071.1, 2054.5, 2024.8	2070.3	1.0229	1.0008	Co(CO) ₂ (NO)
2042.7	1996.6	2042.7	2042.7		2042.7			site
2039.4	1993.4	2039.4	2039.3	2039.4, 2016.0, 2003.2, 1993.4	2039.4	1.0231	1.0000	Co(CO) ₃ (NO)
2026.6	1980.7	1980.7				1.0232		OCoCO
2020.0	1974.5	2019.8	2019.7	2020.1, 1974.6	2019.8			?
2012.4	1967.4	2012.8	2012.5		2012.6			Co(CO)[NO]
2010.1	1965.7	2010.1	2010.1	2010.1, 1989.8, 1965.7	2009.9	1.0226	1.0000	Co(CO) ₂ [NO]
2000.9	1956.4	1999.5	1998.4	2000.8, 1956.3	2000.6	1.0227	1.0007	Co(CO)(NO)
1996.2	1951.4	1996.2	1996.1	1996.2, 1967.4, 1951.4	1996.1	1.0230	1.0000	Co(CO) ₂ (NO)
1983.3	1938.8	1883.3	1983.3		1983.2	1.0229		Co(CO) ₃
1960.5	1913.3	1960.5	1960.5	1960.5, 1913.3	1960.5	1.0247		Co(CO) site
1957.2	1910.1	1917.2	1957.2	957.2, 1910.1	1957.2	1.0247		Co(CO)
1953.0	1908.4	1953.0	1953.0	1952.9, 1908.4	1953.0	1.0234		Co(CO) site
1920.8	1877.7	1920.8	1920.8	1920.8, 1895.0, 1877.7	1920.7	1.0230		Co(CO) ₂
1895.4	-	1895.3	1895.3		1895.3			?
1871.8	1871.8	1839.0	1789.3	1871.8	1871.8, 1839.0		1.0178	NO
1863.3	1863.2	1830.4	1781.2				1.0180	(NO) ₂
1854.9	1852.2	1854.9	1854.8					?
1846.0	1845.9		1769.3					XCoNO
1818.3	1816.5	1783.4	1744.6	1818.9	1818.3, 1783.0	1.0010	1.0196	Co(CO) ₃ (NO)
1814.4	1814.2	1773.5				1.0001	1.0231	Co(NO) ₃
1787.9	1787.9	1752.5	1714.5	1787.2		1.0000	1.0202	Co(CO) ₂ (NO)
1776.1	1776.1	1744.2	1697.4		1776.1, 1757.5, 1744.2		1.0183	(NO) ₂
1770.1	1770.1	1735.3	1696.5		1770.0, 1757.4, 1744.5, 1735.4		1.0201	Co(NO) ₃
1767.9	1766.3	1733.0	1695.4	1767.8, 1766.2	1767.8, 1732.9	1.0009	1.0201	Co(CO)(NO)
1764.8	1764.7	1729.6	1690.4					site
1761.1	1761.3	1724.1					1.0215	Co(NO)
1752.4	1752.4	1718.2	1678.3		1752.4, 1732.9, 1718.2	1.0000	1.0199	Co(CO)(NO) ₂
1737.6	1737.6	1702.6	1665.0		1737.5, 1716.0, 1702.5		1.0206	Co(NO) ₂
1719.7	1719.7	1687.8	1645.4		1719.5, 1699.5, 1687.7	1.0000	1.0189	Co(CO)(NO) ₂
1654.0	1653.9	1623.9	1581.7		1651.7, 1625.6	1.0001	1.0179	Co ₂ (CO) ₃ (NO) ₂
1346.7	1346.7	1323.5	1288.3		1346.6, 1324.0	1.0000	1.0175	Co(CO) ₂ [NO]
1324.1	1323.9	1301.6	1268.0	1324.0	1324.0, 1301.6	1.0001	1.0173	Co(CO)[NO]
1284.2	1284.2	1262.0	1228.5		128344, 1262.0		1.0176	Co[NO]
971.0	971.0	971.0	933.6					OCo(NCO)
948.1			909.0					?
933.5								OCo(NCO)
846.2	846.2	846.2	808.6					CoO
570.5	564.4	560.4	558.7			1.0108	1.0180	Co(CO) ₃ (NO)
474.0	470.1	473.5	472.3			1.0083	1.0011	Co(CO) ₃ (NO)
464.2	459.5	463.9	464.3			1.0102	1.0006	Co(CO) ₂ (NO) or Co(CO)(NO) ₂

¹⁵N¹⁸O isotopic ratios 1.0179 and 1.0282, which are in excellent agreement with the observed values (1.0176 and 1.0275). The 1284.1 cm⁻¹ band decreases slightly on first annealing to 20 K, while the 1324.1 cm⁻¹ band increases, and a new 1346.7 cm⁻¹ band appears. The sharp 1324.1 cm⁻¹ band shifts 0.2 cm⁻¹ with ¹³CO, suggesting association with CO, and gives almost the same ¹⁴NO/¹⁵NO and ¹⁵N¹⁶O/¹⁵N¹⁸O ratios (1.0173 and 1.0265) as Co[NO]. This band appears as sharp doublet absorptions with ^{14,15}NO and ¹⁵N^{16,18}O precursors, so a single NO submolecule is involved. A stronger 2012.4 cm⁻¹ band (0.051 to 0.022 au at 1324.1 cm⁻¹) is associated by marked

growth on annealing and 20% growth on full-arc photolysis (Figure 1).

Our DFT calculations substantiate this assignment in predicting 2010.6 and 1458.1 cm⁻¹ C–O and N–O fundamentals of 3:1 relative intensity. Note again that the C–O mode is predicted accurately, but the N–O mode is too high, this time by 134 cm⁻¹, which is systematic error for the DFT calculation of nitrosyl frequencies, particularly the side-bound species.

OCoNCO. Two bands at 2250.1 and 971.0 cm⁻¹ track together (15:1 relative intensity). These bands appeared on

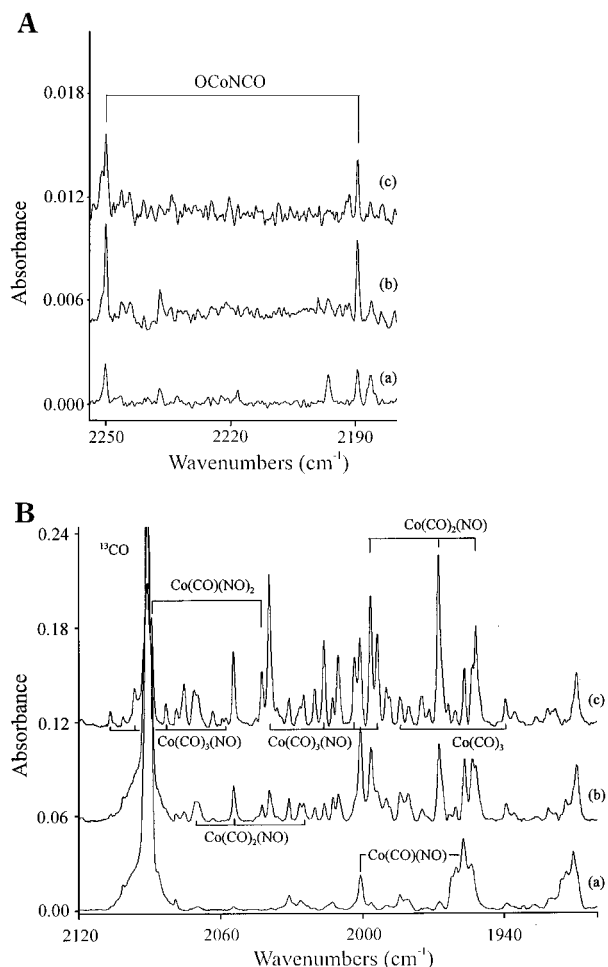


Figure 2. Infrared spectra in the (A) 2255–2180 and (B) 2120–1900 cm^{-1} regions for laser-ablated Co atoms co-deposited with 0.1% ^{12}CO + 0.1% ^{13}CO + 0.2% NO in argon at 7 K: (a) after 1 h sample deposit, (b) after annealing to 30 K, (c) after annealing to 40 K.

deposition, slightly increased on annealing to 20 K, and greatly increased on annealing to 30 and 35 K. The 2250.1 cm^{-1} absorption shows a doublet pattern in both $^{12,13}\text{CO}$ + NO and CO + $^{14,15}\text{NO}$ experiments, giving large 1.0277 $^{12}\text{C}/^{13}\text{C}$ and small 1.0059 $^{14}\text{N}/^{15}\text{N}$ isotopic ratios, respectively, which are slightly higher than CO but lower than NO fundamental isotopic ratios. This absorption is assigned to an N–C–O antisymmetric stretching vibration and is near values for NCO species on catalyst surfaces.⁸ The 971.0 cm^{-1} band shifts to 933.6 cm^{-1} in CO + $^{15}\text{N}^{18}\text{O}$ experiments, but exhibits no ^{13}C and ^{15}N shifts, and the 16/18 ratio, 1.040, is appropriate for a Co–O stretching mode. The CoO molecule absorbs at 846.2 cm^{-1} in solid argon.²⁶ These bands can be assigned to the isocyanate OCoNCO; the weaker symmetric N–C–O mode was not observed. Analogous absorptions have been observed for OMnNCO and OFeNCO.^{11,12}

This identification is supported by the DFT calculations, and the results are summarized in Table 3. The calculated frequencies at 2226.8 and 976.3 cm^{-1} , isotopic ratios, and relative intensities match the experimental values very well.

Co(CO)₂(NO). The absorptions at 2071.2, 1996.2, and 1787.9 cm^{-1} observed on deposition increased greatly on annealing to 30 and 40 K, but slightly decreased on photolysis. Both 2071.2 and 1996.2 cm^{-1} bands exhibit the carbonyl stretching isotopic ratios ($^{12}\text{CO}/^{13}\text{CO}$, 1.0229) and gave a sharp 1:2:1 triplet distribution in $^{12,13}\text{CO}$ + NO experiments, indicating that two equivalent carbonyls are involved, and antisymmetric and

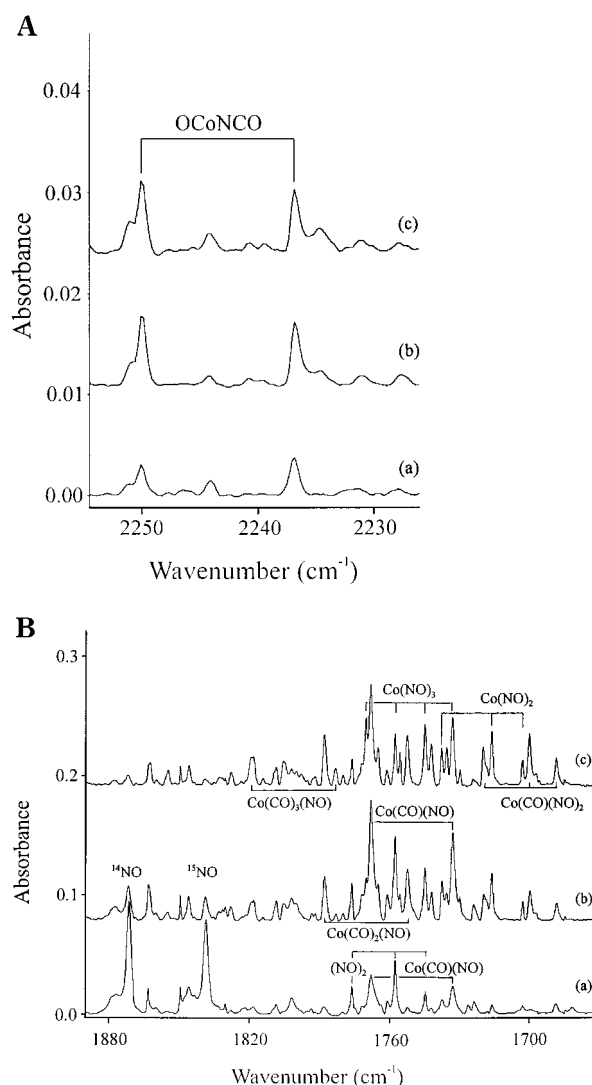


Figure 3. Infrared spectra in the (A) 2255–2230 and (B) 1890–1680 cm^{-1} regions for laser-ablated Co atoms co-deposited with 0.2% CO + 0.1% ^{14}NO + 0.1% ^{15}NO in argon at 7 K: (a) after 1 h sample deposit, (b) after annealing to 30 K, and (c) after annealing to 40 K.

symmetric carbonyl vibrations are observed. The 1787.9 cm^{-1} band shows the nitrosyl stretching isotopic ratio ($^{14}\text{NO}/^{15}\text{NO}$, 1.0202), and a 1:1 doublet was observed in the CO + $^{14,15}\text{NO}$ experiment, which clearly demonstrates one nitrosyl involvement. These three bands are appropriate for the Co(CO)₂(NO) molecule.

Similar DFT calculations done for Co(CO)₂(NO) strongly support this assignment (Tables 2 and 3). The predicted isotopic ratios for both CO and NO stretching vibrations reproduced experimental values very well, and the calculated CO modes are underestimated by 15 and 7 cm^{-1} , respectively, but the NO frequency is overestimated by 54 cm^{-1} .

The same Co(CO)₂(NO) species was observed at 1785, 1997, and 2071 cm^{-1} in early argon matrix experiments from photodissociation of Co(CO)₃(NO).¹³ This transient was also generated by photolysis of Co(CO)₃(NO) and stabilized in liquid xenon by coordination of molecular H₂ or 1-butene to form Co(CO)₂(NO)(H₂)¹⁷ or Co(CO)₂(NO)(η^2 -1-btn),¹⁶ where both CO stretching modes and NO vibration are very close to our argon matrix observations.

Co(CO)₂[NO] or Co(CO)₂(η^2 -NO). A set of bands at 2078.4, 2010.1 and 1346.7 cm^{-1} tracked together, and this trio can be assigned to Co(CO)₂[NO]. These bands appeared on annealing

TABLE 2: Cobalt Carbonyl Nitrosyl States, Relative Energies (kcal/mol), and Geometries Calculated at the BPW91/6-311+G(d) Level

molecule	state	relative energy	geometry (Å, deg)
Co(CO)(NO)	¹ A'	0.0	CoC,1.746; CoN,1.626; CO,1.164; NO,1.175; NCoC,119.3; CoCO,168.7; CoNO,157.7
	³ A''	19.0	CoC,1.782; CoN,1.704; CO,1.161; NO,1.185; NCoC,143.3; CoCO,176.8; CoNO,170.3
Co(CO)[NO]	¹ A	26.0	CoC,1.806; CoN,1.737; CoO,1.883; CO,1.159; NO,1.229; NCoC,178.6; CoCO,173.3
OCoNCO	¹ Σ	26.4	CoO,1.5871; CoN,1.759; NC,1.224; CO,1.174
NCoO(CO)	¹ A	42.5	CoC,1.812; CoN,1.548; CoO,1.598; CO,1.145; NCoC,98.8; CoCO,180.0; NCoO,136.0
OCoOCN	¹ Σ	52.6	CoO,1.581; CoO',1.734; OC,1.255; CN,1.181
Co(CO) ₂ (NO)	¹ A ₁	0.0	CoN,1.644; NO,1.168; CoC,1.812; CO,1.155; CoNO,180.0; CoCO,176.0; CCoC,113.3
	³ B ₁	17.9	CoN,1.719; NO,1.179; CoC,1.820; CO,1.156; CoNO,180.0; CoCO,179.2; CCoC,108.4
Co(CO) ₂ [NO]	¹ A	14.5	CoN,1.777; CoO,1.931; CoC,1.764; CoC',1.823; NO,1.227; CO,1.157; C'O',1.153; NCoO,38.4; CoCO,177.7; CoC'O',171.7; CCoC',99.1
	² B ₁		CoC,1.800; CO,1.155; CoN,1.674; NO,1.171; CoCO,180.0; NCoN,135.2
Co(CO) ₃ (NO)	¹ E		CoN,1.665; CoC,1.811; NO,1.165; CO,1.154; CoNO,180.0; CoCO,178.6; NCoC,115.8; CCoC,102.5

TABLE 3: Stretching Frequencies (cm⁻¹) and Intensities for Isotopic C–O and N–O Vibrations Calculated at the BPW91/6-311+G(d) Level for Ground State Cobalt Carbonyl Nitrosyls

molecule	mode	¹² CO, ¹⁴ NO	¹³ CO, ¹⁴ NO	¹² CO, ¹⁵ NO	(¹² CO/ ¹³ CO)	¹⁴ NO/ ¹⁵ NO
Co(CO)(NO)	C–O	2000.2(591)	1954.7(496)	1998.7(632)	1.0233	1.0008
	N–O	1807.0(984)	1805.0(1033)	1771.3(911)	1.0011	1.0202
Co(CO)[NO]	C–O	2010.6(895)	1963.5(840)	2010.5(898)	1.0240	1.0000
	N–O	1458.1(306)	1458.0(308)	1432.3(294)	1.0000	1.0180
OCoN(CO)	C–O	2104.5(529)	2055.1(499)	2104.5(529)	1.0240	1.0000
	Co–N	1055.6(88)	1055.6(89)	1030.8(97)	1.0000	1.0241
	Co–O	933.6(44)	933.6(44)	929.7(34)	1.0000	1.0042
OCoNCO	N–C–O, a	2226.8(1402)	2164.7(1341)	2217.6(1368)	1.0287	1.0041
	N–C–O, s	1400.4(70)	1400.3(68.3)	1370.9(73)	1.0000	1.0215
	Co–O	976.3(97)	976.3(97)	976.3(97)	1.0000	1.0000
OCoONC	N–C–O, a	2184.0(5)	2127.1(4)	2162.4(4)	1.0268	1.0099
	N–C–O, s	1245.4(80)	1245.9(81)	1233.6(82)	1.0000	1.0096
	Co–O	987.2(86)	987.1(85)	986.9(84)	1.0001	1.0003
Co(CO) ₂ (NO)	C–O, s	2056.3(239)	2009.8(178)	2055.1(273)	1.0231	1.0006
	C–O, a	1989.2(1407)	1943.6(1324)	1989.2(1409)	1.0235	1.0000
	N–O	1841.6(1134)	1840.0(1171)	1804.8(1061)	1.0009	1.0204
Co(CO) ₂ [NO]	C–O, s	2054.2(499)	2006.0(470)	2054.2(500)	1.0240	1.0000
	C–O, a	2000.8(972)	1954.2(915)	2000.8(972)	1.0238	1.0000
	N–O	1450.1(367)	1450.0(369)	1424.2(355)	1.0000	1.0182
Co(CO)(NO) ₂	C–O	2034.6(610)	1989.5(502)	2033.0(656)	1.0227	1.0008
	N–O, s	1846.2(558)	1844.0(618)	1809.9(478)	1.0012	1.0201
	N–O, a	1802.1(1510)	1802.1(1511)	1766.0(1473)	1.0000	1.0204

TABLE 4: Calculated and Experimental Frequencies, Intensities, and Isotopic Frequency Ratios at the BPW91/6-311+G(d) Level for Co(NO)₃(CO) (¹E) in C_{3v} Symmetry

calculated			experimental			
frequencies (cm ⁻¹)	¹² C/ ¹³ C	¹⁴ N/ ¹⁵ N	frequencies (cm ⁻¹)	¹² C/ ¹³ C	¹⁴ N/ ¹⁵ N	assignment
2076.7(168) ^a	1.0234	1.0005	2106.8 ^c	1.0231	1.0004	CO str, sym
2015.5(934 × 2) ^b	1.0238	1.0000	2039.4	1.0231	1.0000	CO str, asym
1852.8(1124)	1.0002	1.0203	1818.3	1.0010	1.0196	NO str
618.9(9)	1.0005	1.0070				Co–N str
595.0(63 × 2)	1.0100	1.0164	570.5	1.0108	1.0180	CoNO bend
510.5(22 × 2)	1.0243	1.0024				Co–C str
492.7(61)	1.0318	1.0008	474.0	1.0083	1.0011	CoCO bend
473.3(6 × 2)	1.0218	1.0000				
423.9(0.4)	1.0146	1.0014				
326.0(0)	1.0316	1.0000				
297.6(0.2 × 2)	1.0220	1.0088				
85.6(0)	1.0017	1.0000				
78.0(0.1 × 2)	1.0026	1.0000				
60.0(0 × 2)	1.0034	1.0000				

^a Mode a₁ symmetry. ^b Mode e symmetry × 2 intensity. ^c Absorbances in a.u. after 40 K annealing: 2106.8(0.030), 2039.4(0.19), 1818.3(0.083), 570.5(0.013), 474.0(0.008).

to 20 K, tripled on annealing to 30 K, while the 1324.1 cm⁻¹ band only doubled, decreased on λ > 470 nm and increased on λ > 240 nm photolysis and increased again on further annealing to 35 and 40 K, which is unique behavior in this system. The 2010.1 and 2078.4 cm⁻¹ bands show typical ¹²CO/¹³CO isotopic ratios of 1.0234 and 1.0226, respectively, and the intensity ratio of lower to upper is about 2:1. The mixed ^{12,13}CO + NO spectra exhibit one intermediate peak for the 2010.1 cm⁻¹ feature, but band overlap complicates the spectrum. The 1346.7 cm⁻¹ band shows no ¹³CO isotopic shift, but shifts to 1323.5 cm⁻¹ in CO + ¹⁵NO spectra and exhibits a 1:1 doublet pattern in CO + ^{14,15}NO spectra. The 1.0175 ¹⁴NO/¹⁵NO isotopic ratio of this

band is very close to the ¹⁴NO/¹⁵NO ratio for side-on metal nitrosyls. This band is assigned to the NO stretching vibration of Co(CO)₂[NO].

Similar DFT calculations were done for this complex, and the results are listed in Tables 2 and 3. The calculations predicted two inequivalent end-on CO and one side-on NO for this molecule. The calculated isotopic ratios match the experimental values very well, and CO stretching modes are only 24.2 and 9.3 cm⁻¹ lower, respectively. However, the predicted NO stretching mode is 103.4 cm⁻¹ higher, more discrepancy than for the end-on NO frequencies. It is noted that the side-on NO

frequencies were overestimated in $\text{Fe}(\text{CO})_x[\text{NO}]$, $\text{Mn}(\text{CO})_x[\text{NO}]$, and other side-on metal nitrosyls by density functional calculations.^{20,27–32}

Co(CO)(NO)₂. The absorptions at 2089.0, 1752.4, and 1719.7 cm^{-1} behaved similarly. They appeared in the spectra after first annealing to 20 and 30 K, and became stronger on annealing to 35 and 40 K. The isotopic substitution produced 1.0227 ¹²C/¹³C ratio for 2089.0 cm^{-1} band, and 1.0199 and 1.0189 ¹⁴N/¹⁵N ratios for 1752.4 and 1719.7 cm^{-1} bands, respectively. The first band produced a doublet with ^{12,13}CO + NO, and the last band gave a 1:2:1 triplet with CO + ^{14,15}NO, but the structure for the 1752.4 cm^{-1} band could not be resolved due to band overlap. This evidence provides a convincing case for assignment of these three bands to the $\text{Co}(\text{CO})(\text{NO})_2$ molecule.

The DFT calculations predict the CO stretching mode to be 2.6% lower, and two NO stretching modes 5% higher than the observed bands, which supports this assignment. Again, we note the systematic discrepancies.

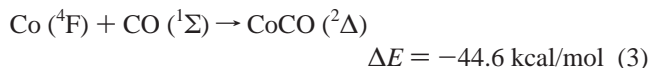
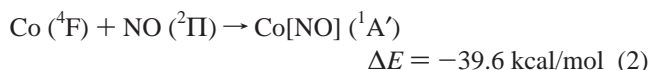
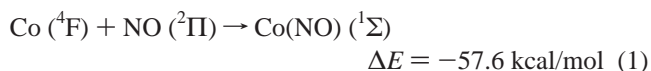
Co(CO)₃(NO). A group of bands at 2106.8, 2039.4, 1818.3 cm^{-1} in CO and NO stretching region and 570.5, 474.0 cm^{-1} in lower region track together, and are due to the saturated $\text{Co}(\text{CO})_3(\text{NO})$ molecule, which are in accord with C_{3v} structure and theoretical calculations. The upper 2039.4 cm^{-1} band shows a quartet shape in ^{12,13}CO + NO experiments, with a 1.0231 ¹²C/¹³C isotopic ratio, which is appropriate for symmetric vibration of three equivalent CO subunits. The 2106.8 cm^{-1} band tracks with the 2039.4 cm^{-1} band and gives ¹²C/¹³C, 1.0255 isotopic ratio, but unfortunately the ^{12,13}CO + NO spectra were overlapped. The strong band at 1818.3 cm^{-1} goes together with the upper bands and shows doublet shape in CO + ^{14,15}NO experiments and 1.0196 ¹⁴N/¹⁵N isotopic ratio all indicating one NO subunit. These three upper bands are very close to the gas-phase $\text{Co}(\text{CO})_3(\text{NO})$ spectrum¹⁵ at 2110, 2040, and 1825 cm^{-1} and argon matrix bands¹³ at 2106, 2040, and 1819 cm^{-1} . In addition two new bending absorptions at 570.5 and 474.0 cm^{-1} are observed here for $\text{Co}(\text{CO})_3(\text{NO})$.

The DFT calculations of frequencies, isotopic ratios, vibrational mode assignments, and experimental observations for $\text{Co}(\text{CO})_3(\text{NO})$ are summarized in Table 4. The very strong CO antisymmetric and weak CO symmetric stretching modes are predicted at 2015.5 and 2076.7 cm^{-1} , which are only 23.9 and 30.1 cm^{-1} lower than observed values, while the NO stretching mode is overestimated by 34.5 cm^{-1} . Furthermore, the calculated isotopic ratios for CO and NO stretching modes are in accord with experimental observations. Calculated CoNO and CoCO bending modes at 595.0 cm^{-1} (¹⁴NO/¹⁵NO, 1.0164) and 492.7 cm^{-1} (¹⁴NO/¹⁵NO, 1.0008) are close to the observed values at 570.5 cm^{-1} (¹⁴NO/¹⁵NO, 1.0180) and 474.0 cm^{-1} (¹⁴NO/¹⁵NO, 1.0011). Furthermore, the calculated intensities match the relative observed absorbances very well.

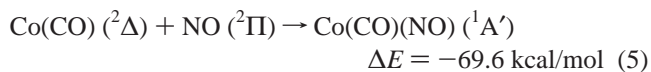
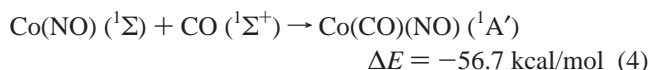
Other Absorptions. There remain several bands to be identified, and most of these increase markedly on final annealings, which suggests higher aggregate species. The broader 1654.0 cm^{-1} band is a case in point: the ^{14,15}NO experiment produced a broader 1651.7–1625.6 cm^{-1} doublet, inside of the pure ¹⁴NO and ¹⁵NO components, which indicate the involvement of at least two NO subgroups. The 1846.0 cm^{-1} band was observed in our earlier Co + NO experiments where it showed evidence of a single NO subunit and the present spectra are in accord. As this band continues to increase on late annealing after CoNO at 1761.1 cm^{-1} decreases, it appears to be a higher single NO species, and OCoNO was suggested. The dimetal CoCo species is also a possibility. We note that dicobalt carbonyls increase markedly on 30 K annealing in our

carbonyl experiments.¹⁹ The weak 2026.6 cm^{-1} band is due to OCoCO, also observed in the Co reaction with CO_2 .³³

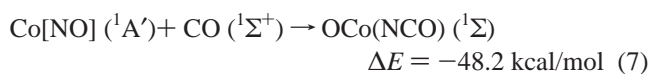
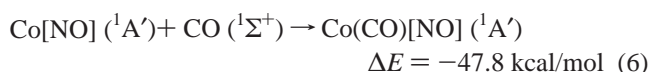
Reaction Mechanisms. In the laser-ablation Co reaction with NO in excess argon and neon, both end-on and side-on cobalt nitrosyls are produced by direct reactions during matrix deposition and on annealing,²⁰ and CoCO is formed in the analogous reactions with CO.¹⁹



The cobalt carbonyl nitrosyl $\text{Co}(\text{CO})(\text{NO})$ appeared on sample deposition and increased on first 20 K annealing from the reaction of $\text{Co}(\text{NO})$ with CO or $\text{Co}(\text{CO})$ with NO.



On 20 K sample annealing the $\text{Co}[\text{NO}]$ absorption decreased while $\text{Co}(\text{CO})[\text{NO}]$ and $\text{OCo}(\text{NCO})$ increased. The exothermic reactions of CO with $\text{Co}[\text{NO}]$ are straightforward; rearrangement to the slightly more stable isocyanate species with separated N and O also occurs on annealing. This is a significant result as experimental evidence shows that side-on $\text{Co}[\text{NO}]$ reacts with CO to break the NO bond and produce the isocyanate, $\text{OCo}(\text{NCO})$, and the reaction requires little activation energy and is thermodynamically favorable. However, the bare cobalt metal atom does not break open the NO bond in laser-ablated Co reactions even after photolysis.²⁰ It appears that formation of precursor, $\text{Co}[\text{NO}]$, is critical for the isocyanate

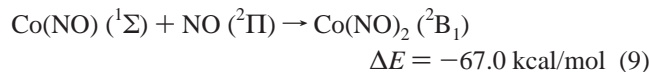
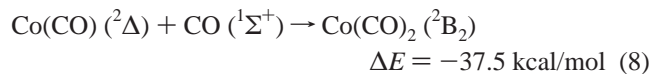


reaction. Although it is possible for CoCO to react with NO to produce $\text{OCo}(\text{NCO})$, this reaction is 26.4 kcal/mol less exothermic than reaction 5 and provides poor competition.

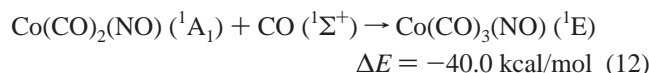
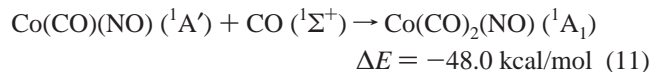
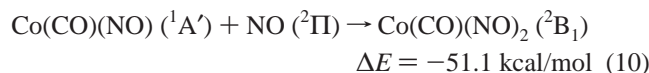
The similar reactions have been performed for iron and manganese with CO and NO mixtures in this laboratory.^{11,12} The $\text{OFe}(\text{NCO})$ and $\text{OMn}(\text{NCO})$ isocyanates were observed on sample photochemical isomerizations, but the $\text{M}(\text{CO})[\text{NO}]$ were produced from visible photolysis of $\text{M}(\text{CO})(\text{NO})$, which rearrange to $\text{OM}(\text{NCO})$ ($\text{M} = \text{Fe}, \text{Mn}$) by subsequent ultraviolet photolysis. Photolysis is not required for the formation of $\text{OCo}(\text{NCO})$ in these experiments.

The $\text{Co}(\text{CO})_2$ and $\text{Co}(\text{NO})_2$ intermediates are also produced spontaneously on sample annealing as in the previous CO and NO experiments.^{19,20} Reactions 5 and 9 are more exothermic, which suggest that the $\text{Co}(\text{CO})(\text{NO})$ molecule is produced at the expense of $\text{Co}(\text{CO})$ while $\text{Co}(\text{NO})$ combined with NO to give $\text{Co}(\text{NO})_2$.

The unsaturated $\text{Co}(\text{CO})_2(\text{NO})$ and $\text{Co}(\text{CO})(\text{NO})_2$ complexes are produced on further sample annealing. Reaction 10 is slightly



more exothermic than reaction 11 since NO with one unpaired electron in a π^* orbital is more reactive than CO. The Co(CO)_3 and Co(NO)_3 species appear as weak bands in the present experiments, and Co(CO)_4 is detected as a weak 2016.6 cm^{-1} band on 35 and 40 K annealing where major growth was observed previously.¹⁹



The stable 18-electron $\text{Co(CO)}_3(\text{NO})$ molecule increased on further annealing, which is less exothermic than reactions 10 and 11. Note that both 18-electron $\text{Fe(CO)}_2(\text{NO})_2$ and $\text{Mn(CO)}_2(\text{NO})_3$ became dominant products on final sample annealing^{11,12} and $\text{Co(CO)}_3(\text{NO})$ did likewise in these experiments.

Conclusions

Several unsaturated cobalt carbonyl nitrosyls were generated by reactions of laser-ablated cobalt atoms with CO and NO mixtures during co-deposition and further reactions on sample annealing and photolysis. The bands at 2000.9 and 1767.9 cm^{-1} are assigned to the CO and NO stretching modes of $\text{Co(CO)}_2(\text{NO})$ based on the ^{13}CO , ^{15}NO , and $^{15}\text{N}^{18}\text{O}$ isotopic shifts, and the spectra of isotopic mixtures. The vibrational frequencies and isotopic ratios of $\text{Co(CO)}_2(\text{NO})$ are reproduced very well by DFT/BPW91 calculations. The $\text{Co(CO)}_2(\text{NO})$ complex produced $\text{Co(CO)}_2(\text{NO})$, $\text{Co(CO)}_2(\text{NO})_2$, and $\text{Co(CO)}_3(\text{NO})$ by coordination of more CO and/or NO. Three side-bonded $\text{Co(CO)}_{0,1,2}\text{-[NO]}$ species were also observed.

The isocyanate OCo(NCO) appears to be produced by the side-on Co[NO] reaction with CO to break the NO bond. This is a significant result as it shows from experimental evidence that this reaction on annealing requires little activation energy and is thermodynamically favorable. However, the bare metal cobalt atom cannot form NCoO in these experiments.²⁰

Acknowledgment. We appreciate financial support from N.S.F. Grant 00-78836 and computer time from the San Diego Supercomputer Center.

References and Notes

(1) Cotton, F. A.; Wilkinson, G.; Murillo, C. A.; Bochmann, M. *Advanced Inorganic Chemistry*, 6th ed.; Wiley: New York, 1999.

- (2) Brown, W. A.; King, D. A. *J. Phys. Chem. B* **2000**, *104*, 2578.
 (3) Ukisu, Y.; Sata, S.; Muramatsu, G.; Yoshida, K. *Catal. Lett.* **1991**, *11*, 177.
 (4) Ukisu, Y.; Sata, S.; Muramatsu, G.; Yoshida, K. *Appl. Catal. B* **1993**, *2*, 147.
 (5) Bell, V. A.; Feeley, J. S.; Deeba, M.; Farruto, R. J. *J. Catal. Lett.* **1994**, *29*, 15.
 (6) Tanaka, T.; Okuhara, T. *Appl. Catal. B* **1994**, *4*, L1.
 (7) Li, C.; Bethke, A.; Kung, H. H.; Kung, M. C. *J. Chem. Soc., Chem. Commun.* **1995**, 813.
 (8) Miners, J. H.; Bradshaw, A. M.; Gardner, P. *Phys. Chem. Chem. Phys.* **1999**, *1*, 4909. Sumiya, S.; He, H.; Abe, A.; Takezawa, N.; Yoshida, K. *J. Chem. Soc., Faraday Trans.* **1998**, *94*, 2217.
 (9) Almusateer, K. A.; Chung, S. S. C. *J. Phys. Chem. B* **2000**, *104*, 2265.
 (10) Gopinath, C. S.; Zaera, F. *J. Phys. Chem. B* **2000**, *104*, 3109.
 (11) Wang, X. F.; Zhou, M. F.; Andrews, L. *J. Phys. Chem. A* **2000**, *104*, 7964 (Mn + CO + NO).
 (12) Wang, X. F.; Zhou, M. F.; Andrews, L. *J. Phys. Chem. A* **2000**, *104*, 10104 (Fe + CO + NO).
 (13) Crichton, O.; Rest, A. J. *J. Chem. Soc., Dalton Trans.* **1977**, 536.
 (14) Fredeen, D. A.; Russell, D. H. *J. Am. Chem. Soc.* **1986**, *108*, 1860.
 (15) Rayner, D. M.; Nazran, A. S.; Drouin, M.; Hackett, P. A. *J. Phys. Chem.* **1986**, *90*, 2882.
 (16) Gadd, G. E.; Poliakoff, M.; Turner, J. J. *Inorg. Chem.* **1986**, *25*, 3604.
 (17) Gadd, G. E.; Upmacis, R. K.; Poliakoff, M.; Turner, J. J. *J. Am. Chem. Soc.* **1986**, *108*, 2547.
 (18) Burkholder, T. R.; Andrews, L. *J. Chem. Phys.* **1991**, *95*, 8697. Hassanzadeh, P.; Andrews, L. *J. Phys. Chem.* **1992**, *96*, 9177.
 (19) Zhou, M. F.; Andrews, L. *J. Phys. Chem. A* **1999**, *103*, 7773 (Co + CO).
 (20) Zhou, M. F.; Andrews, L. *J. Phys. Chem. A* **2000**, *104*, 3915 (Fe, Co, Ni + NO).
 (21) Frisch, M. J.; Trucks, G. W.; Schlegel, H. B.; Gill, P. M. W.; Johnson, B. G.; Robb, M. A.; Cheeseman, J. R.; Keith, T.; Petersson, G. A.; Montgomery, J. A.; Raghavachari, K.; Al-Laham, M. A.; Zakrzewski, V. G.; Ortiz, J. V.; Foresman, J. B.; Cioslowski, J.; Stefanov, B. B.; Nanayakkara, A.; Challacombe, M.; Peng, C. Y.; Ayala, P. Y.; Chen, W.; Wong, M. W.; Andres, J. L.; Replogle, E. S.; Gomperts, R. R.; Martin, L.; Fox, D. J.; Binkley, J. S.; Defrees, D. J.; Baker, J.; Stewart, J. P.; Head-Gordon, M.; Gonzalez, C.; and Pople, J. A. *Gaussian 94*, Revision B.1, Gaussian Inc.: Pittsburgh, PA, 1995.
 (22) Perdew, J. P. *Phys. Rev. B* **1986**, *33*, 8822.
 (23) Becke, A. D. *J. Chem. Phys.* **1993**, *98*, 5648.
 (24) Hay, P. J.; Wadt, W. R. *J. Chem. Phys.* **1985**, *82*, 299.
 (25) Hedberg, K.; Hedberg, L.; Hagen, K.; Ryan, R. R.; Jones, L. H. *Inorg. Chem.* **1985**, *24*, 2771.
 (26) Chertihin, G. V.; Citra, A.; Andrews, L.; Bauschlicher, C. W., Jr. *J. Phys. Chem. A* **1997**, *101*, 8793 (Co + O₂).
 (27) Zhou, M. F.; Andrews, L. *J. Phys. Chem. A* **1998**, *102*, 7452 (Cr + NO).
 (28) Andrews, L.; Zhou, M. F.; Ball, D. W. *J. Phys. Chem. A* **1998**, *102*, 10041 (Mn, Re + NO).
 (29) Zhou, M. F.; Andrews, L. *J. Phys. Chem. A* **1999**, *103*, 478. (V + NO). Zhou, M. F.; Andrews, L. *J. Phys. Chem. A* **1998**, *102*, 10025 (Nb, Ta + NO).
 (30) Kushto, G. P.; Zhou, M. F.; Andrews, L.; Bauschlicher, C. W., Jr. *J. Phys. Chem. A* **1999**, *103*, 478. (Sc, Ti + NO).
 (31) Andrews, L.; Zhou, M. F. *J. Phys. Chem. A* **1999**, *103*, 4167 (Mo, W + NO).
 (32) Zhou, M. F.; Andrews, L. *J. Phys. Chem. A* **2000**, *104*, 2618 (Cu + NO).
 (33) Zhou, M. F.; Liang, B.; Andrews, L. *J. Phys. Chem. A* **1999**, *103*, 2013 (Co + CO₂).